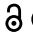



RESEARCH PAPER

 OPEN ACCESS 

Cannabinoid receptors are differentially regulated in the pancreatic islets during the early development of metabolic syndrome

Antonio Barajas-Martínez , Karina Bermeo , Lizbeth de la Cruz , Marina Martínez-Vargas ,
Ricardo Jesús Martínez-Tapia , David Erasmo García  and Luz Navarro 

^aDepartamento de Fisiología, Universidad Nacional Autónoma de México (UNAM), Ciudad de México, México; ^bPrograma de Doctorado en Ciencias Biomédicas, Universidad Nacional Autónoma de México (UNAM), Ciudad de México, México

ABSTRACT

The endocannabinoid system is found in tissues that regulate the glycemia, including adipose tissue, muscle, and pancreatic islets. Diet-induced metabolic syndrome changes the expression of the CB receptors in muscle, adipose tissue, and liver. However, it is poorly understood whether metabolic syndrome (MetS) affects the expression of CB receptors in pancreatic β cells. We analyzed the expression of CB receptors in pancreatic β cells under chronic high-sucrose diet (HSD)-induced MetS. Wistar rats fed an HSD as a model of MetS were used to investigate changes in cannabinoid receptors. After 8 weeks of treatment, we evaluated the appearance of the following MetS biomarkers: glucose intolerance, hyperinsulinemia, insulin resistance, hypertriglyceridemia, and an increase in visceral adiposity. To determine the presence of CB1 and CB2 receptors in pancreatic β cells, immunofluorescence of primary cell cultures and pancreatic sections was performed. For whole-islet quantification of membrane-bound CB1 and CB2 receptors, western-blotting following differential centrifugation was conducted. Our results revealed that an HSD treatment closely mimics the alterations seen in MetS. We observed that in primary cell culture, CB1 and CB2 receptors were expressed at a higher level in pancreatic β cells compared with non- β cells. MetS resulted in a reduction of CB1 in the islet, whereas abundant CB2 was observed after the treatment. CB1 and CB2 receptors are differentially expressed in pancreatic β cells during MetS development.

ARTICLE HISTORY

Received 12 February 2020
Revised 19 October 2020
Accepted 7 November 2020

KEYWORDS



Metabolic syndrome;
endocannabinoid system;
hyperinsulinemia; insulin
resistance; cannabinoid
receptors

Introduction

The endocannabinoid system (ECS) is widely distributed throughout the body and is present in several locations, including the brain, heart, immune system, and bone.¹ It is found in organs and tissues involved in the regulation of the glycemic control, such as the hypothalamus in the central nervous system, as well as in peripheral organs, including adipose tissue, liver, muscle,^{2,3} and pancreas, specifically in the pancreatic islets.⁴ ECS provides a negative feedback loop that modulates cellular responses to stimuli.⁵ Indeed, cannabis consumption has been linked with increased palatable food intake,⁶ lipogenesis promotion,⁷ and decreased glucose tolerance.⁸ Conversely, cannabinoid antagonists display opposite effects.⁹ However, previous epidemiological studies consistently reported a decrease in the incidence of diabetes in cannabis consuming populations,¹⁰ even after considering several confounding factors.¹¹ This finding highlights the relevance of long-term changes in the ECS system.

In pancreatic β cells, endocannabinoids are synthesized in response to glucose stimulation and membrane depolarization by Ca^{2+} -dependent enzymes.^{4,12} Endocannabinoids have been proposed as an autocrine or paracrine signaling system in the pancreatic islet cells. They activate CB1 and CB2 receptors, which are coupled to $G_{i/o}$ proteins.¹³ This endogenous activation decreases the intracellular cAMP concentration, calcium oscillations, and insulin release.^{12,14} Furthermore, the activation of CB1 inhibits voltage-gated calcium channels.¹⁵ CB1 and CB2 receptor activation decreases calcium oscillations, which in turn diminishes insulin release,^{16,17} causing glucose intolerance.⁸

In order to better understand the interplay between cannabinoids and the development of diabetes, it is necessary to know whether cannabinoid receptors are dysregulated in pancreatic islets. A similar dysregulation could be found in metabolic syndrome (MetS), as a leading risk factor for diabetes development.¹⁸ Several reports about the effects of cannabinoid compounds show short-term

CONTACT Luz Navarro  lnavarro@unam.mx  Departamento de Fisiología, Universidad Nacional Autónoma de México (UNAM), Ciudad de México C.P. 04510, México.

© 2020 The Author(s). Published with license by Taylor & Francis Group, LLC.
This is an Open Access article distributed under the terms of the Creative Commons Attribution-NonCommercial-NoDerivatives License (<http://creativecommons.org/licenses/by-nc-nd/4.0/>), which permits non-commercial re-use, distribution, and reproduction in any medium, provided the original work is properly cited, and is not altered, transformed, or built upon in any way.

modulation of pancreatic islet function by CB1 and CB2 receptors.¹⁹ Notably, MetS-inducing diets alter mRNA expression for cannabinoid receptors in muscle,²⁰ and adipose tissue.²¹ In pancreatic islets, the expression of the CB1 cannabinoid receptor is decreased acutely after glucose administration.¹⁶ Furthermore, increased levels of endocannabinoids have been found in pancreatic islets of mice fed with a high-fat diet.²² Nonetheless, CB1 and CB2 receptor changes have not been investigated in a high-sucrose diet (HSD)-induced MetS. Therefore, the purpose of this work was to investigate the expression of CB1 and CB2 receptors in pancreatic islets from rats with MetS.

Results

Glucose dysregulation induced by an HSD

To assess the metabolic status induced in rats after 8 weeks of HSD, several biomarkers of MetS were measured. The weight, body fat, and visceral fat pads were all increased following an HSD regimen (Table 1, Figure 1A). Weight and body composition changes were accompanied by elevations of MetS biomarkers, such as fasting hyperinsulinemia (control 1.4 ± 0.2 ng/mL vs. treatment 5 ± 0.8 ng/mL, $p < .001$) and fasting hypertriglyceridemia (control 135 ± 7 mg/dL vs. treatment 220 ± 11 mg/dL) without differences in fasting glucose (Figure 1B–D). Insulin resistance estimation by HOMA-IR was increased in the HSD group (control 1.8 ± 0.3 A.U. vs. treatment 6.4 ± 1.4 A.U.) (Figure 1E). *In vivo*

glucose homeostasis was assessed by plasma glucose levels after a glycemic challenge (intraperitoneal glucose tolerance test, IPGTT) and an insulin challenge (insulin tolerance test, ITT). Triglyceride levels in response to these challenges were recorded. IPGTT results showed glucose intolerance in the treated group. HSD serum glucose levels were significantly higher at the glycemic peak in the 15 min (control 143 ± 3 mg/dL vs. treatment 220 ± 18 mg/dL, $p < .001$) and 30 min (control 129 ± 5 mg/dL vs. treatment 169 ± 11 mg/dL, $p < .05$) (Figure 1F). Following the insulin tolerance test (ITT), the percentage decrease in the glucose level was the same for both groups, with the lowest value reached 60 min after administration. The control and the treated group reached mean reductions of 67% and 69%, respectively, with no statistically significant difference. However, at the end of the test, the mean glucose reduction reached a plateau at 68% in the control group, while it returned to the original glucose level in the treated group, with an SEM difference of $\pm 12\%$, suggesting a faster recovery from the hypoglycemic condition (Figure 1G). The triglyceride response to the glycemic challenge showed a prolonged response during the third hour of the test (control 117 ± 9 mg/dL, 108% increase vs. treatment 216 ± 28 mg/dL, 141% increase, $p < .05$) (Figure 1H). Fasting hyperinsulinemia and hypertriglyceridemia, accompanied by increased visceral fat pad deposits, are characteristic of MetS. We found that 8 weeks of an HSD impaired glucose tolerance without decreasing insulin sensitivity, as shown by the ITT, with a greater recovery of the glycemia in

Table 1. Body composition changes in MetS induced by HSD.

| | Bioimpedance estimated mass (g) | | | |
|-----------------------------------|---------------------------------|-----------------------|-----------------------|---------|
| | Control mean \pm S.E.M. | HSD mean \pm S.E.M. | Difference \pm S.E. | p Value |
| Body weight** | 407.7 \pm 10.7 | 468 \pm 18.5 | 60.3 \pm 17.2 | <.01 |
| Body fat * | 146.2 \pm 8.1 | 191.4 \pm 8.6 | 45.2 \pm 15.3 | <.05 |
| Fat free mass ^{ns} | 218.2 \pm 7.6 | 248.6 \pm 6.4 | 30.4 \pm 15.3 | .2 |
| Extracellular water ^{ns} | 106.2 \pm 15.6 | 79.4 \pm 7.8 | –26.8 \pm 21.1 | .3 |
| Total body water ^{ns} | 253.8 \pm 36.4 | 210.5 \pm 13.4 | –43.3 \pm 21.1 | .2 |
| | Visceral fat pads weight (g) | | | |
| | Control mean \pm S.E.M. | HSD mean \pm S.E.M. | Difference \pm S.E. | p Value |
| Pericardial ^{ns} | 0.2 \pm 0.04 | 0.6 \pm 0.1 | 0.4 \pm 0.6 | .5 |
| Peripancreatic * | 0.9 \pm 0.1 | 2.2 \pm 0.3 | 1.3 \pm 0.5 | <.05 |
| Epididymal *** | 2 \pm 0.3 | 5 \pm 0.5 | 3 \pm 0.5 | <.001 |
| Retroperitoneal *** | 2 \pm 0.3 | 5.6 \pm 0.6 | 3.6 \pm 0.6 | <.001 |

For comparing differences between diet groups, bioimpedance estimates of body composition are presented above and visceral fat pads weight below. All results are presented as mean \pm SEM, and differences were computed through multiple t-tests with Holm-Sidak correction for multiple comparisons. Significance levels are presented as follows * $p < 0.05$, ** $p < 0.01$, *** $p < 0.001$. The HSD group had increased weight due to body fat, an increase mostly reflected in the visceral fat pad (Peripancreatic, epididymal, and retroperitoneal fat pads).

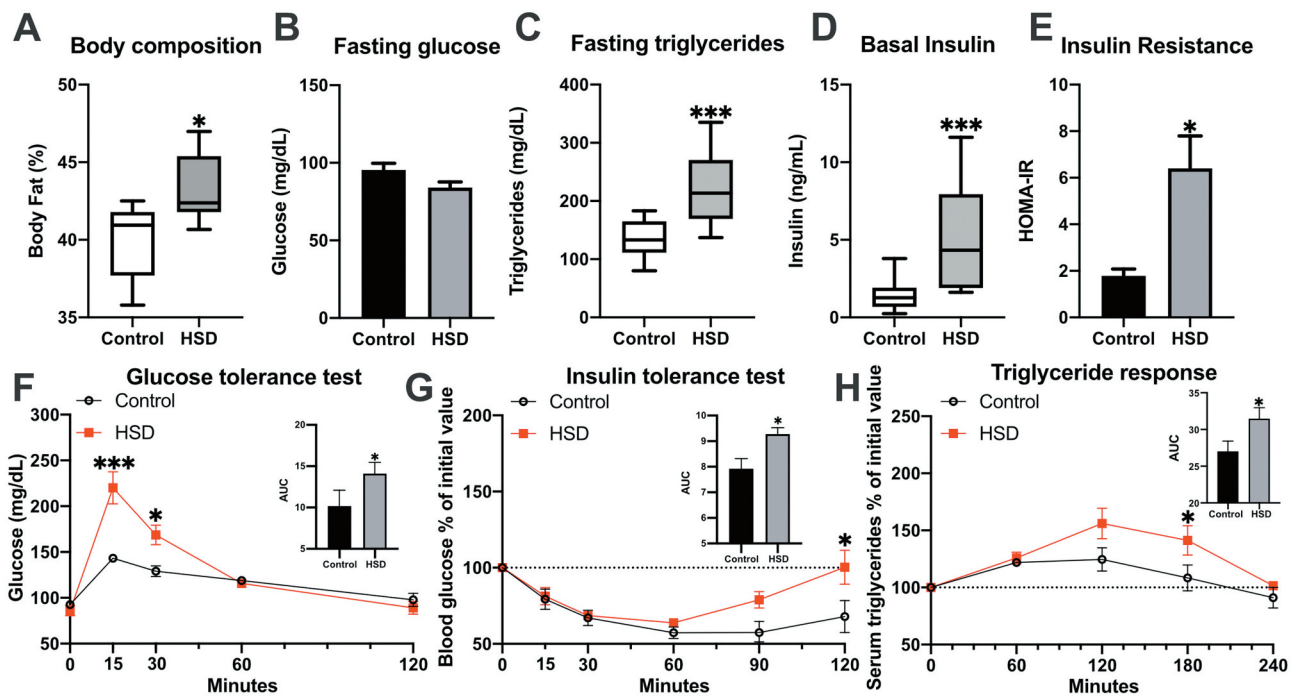


Figure 1. Glucose regulation is altered in the high-sucrose diet model of MetS.

Body fat percentage (A), fasting levels of glucose (B), insulin (C), triglycerides (D), and insulin resistance (E) are shown. (F) shows the intraperitoneal glucose tolerance test differences between groups at 15 and 30 min after the intraperitoneal administration of a 1 g/kg glucose challenge. (G) presents the percentage reduction in fasting glucose levels after insulin administration, with a recovery of glucose levels only observed in the HSD group. The increase in triglyceride response in the HSD group to the glucose challenge is shown in (H). Variables with normal distribution are presented as bars with mean \pm SEM, and were compared with a t-test. Variables with non-normal distribution are presented as Tukey box-plots with median, interquartile range (IQR), and whiskers for the 1.5 IQR range, and were compared with Mann-Whitney tests. Time-dependent variables were compared by two-way ANOVA followed by Bonferroni *post hoc* test. AUC was calculated and compared with t-tests and is presented as mean \pm SEM. Significance levels are presented as follows * $p < .05$, ** $p < .01$, *** $p < .001$.

the treated group and an increased triglyceride response to the hyperglycemic challenge.

Cannabinoid receptor expression in primary culture from dissociated islets

Immunofluorescence of a primary culture from dissociated islets from control rats was carried out to identify the cell populations that expressed CB1 and CB2 receptors. Insulin-positive cells were the most abundant in the islet primary cultures, accounting for 73% of the total cell population. Pancreatic β cells had a distinctive diameter of $12 \pm \text{SD } 2 \mu\text{m}$ and granular cytoplasm. Besides, most of the insulin-negative cells, which represented 26% of the culture, where morphologically recognizable as α -cells. They had a smaller diameter averaging $7.5 \pm \text{SD } 1 \mu\text{m}$ with uniform round nuclei and coarsely clumped chromatin. Other cell populations that were neither insulin- nor glucagon-positive, such as fibroblasts, were also observed. Both CB1 and CB2 receptors were present

in the main cell populations of the islet, both β and non- β cells (Figure 2A,C). The fluorescence signal indicated an increased abundance of cannabinoid receptors in β cells relative to non- β cells, for both CB1 (mean difference of 12 ± 2 arbitrary units (A.U.), $p < .001$), and CB2 (mean difference of 33 ± 3 A.U., $p < .001$) in primary culture conditions (Figure 2B,D).

Cannabinoid receptors in pancreatic islets are dysregulated in MetS

To determine whether MetS changes the density of CB1 and CB2 receptors in the pancreatic islets, immunofluorescence of pancreatic sections was conducted. CB1 was decreased in the pancreatic islets of rats with MetS (Figure 3A). This decrease occurred both in β cells (mean difference -10.5 ± 4 A.U., $p < .001$) and non- β cells (mean difference -32 ± 4 A.U., $p < .001$) (Figure 3B). In contrast, for CB2 the fluorescence amount in the MetS group increased both in β (mean difference 7.5 ± 1 A.U., $p < .001$) and

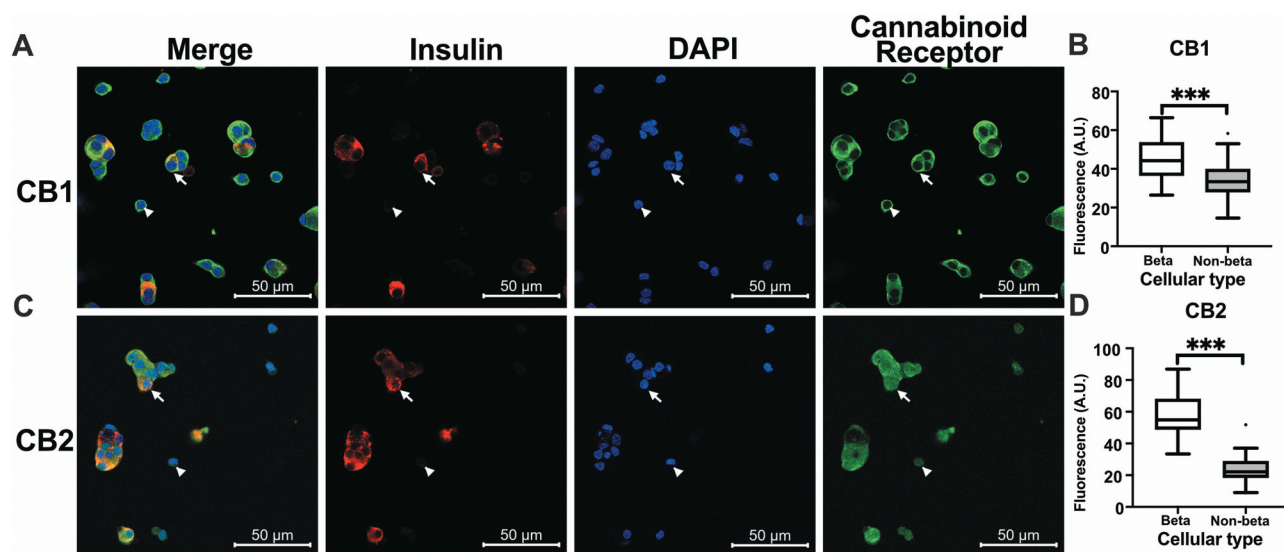


Figure 2. Cannabinoid receptor expression in dissociated primary culture.

Primary islet culture from control islets immunofluorescence showed the presence of cannabinoid in (A) for CB1 and (C) for CB2. The first column shows the merged image. Pancreatic β cells are identified by the insulin presence in red. The cannabinoid receptor is shown in green. For cellular identification, the DAPI-stained nucleus in blue is presented in the third column. Arrows indicate representative β cells, and non- β cells are indicated with arrowheads. Corrected fluorescence (see methods) for CB1 is presented in (B), and for CB2 in (D). Results are presented as Tukey box-plots with outliers and were compared with Mann-Whitney tests. Significant results are shown as *** $p < .001$.

in non- β cells (mean difference 10 ± 2 A.U., $p < .001$) (Figure 3C,D). Markedly, non- β cells had greater levels of CB1 fluorescence than β cells in the control group (mean difference 21.3 ± 3.5 A.U., $p < .001$), while non- β cells had greater levels of CB2 fluorescence than β cells in the HSD group (mean difference 6 ± 1.4 A.U., $p < .01$). Next, we proceeded to determine whether these changes were reflected in the total amount of membrane-bound receptors. For the membranal protein fraction of CB1, a mean difference of -2.6 ± 0.5 A.U. ($p < .01$) was found, whereas for the membrane-bound CB2 protein fraction showed a mean difference of 1 ± 0.3 A.U. ($p < .05$). As expected, both proteins resulted in the molecular weight reported for these receptors (Figure 3E,F). The amount of membrane-bound receptors and the total receptors showed similar trends. Thus, CB1 expression decreased while CB2 expression increased in the pancreatic islet. Furthermore, this change was observed for both β and non- β cells.

Discussion

Cannabinoid receptors and their functional expression have been objects of pharmacological studies as

they might be therapeutic targets for glycemic control. To date, most of the reports were conducted in either cellular cultures or whole-islets. Interestingly, we found a differential expression of CB receptors in whole-islets and cultured dissociated cells. In whole-islets both cannabinoid receptors were predominantly expressed in non- β cells, CB1 in control and CB2 in HSD conditions (Figure 3). In contrast, although both CB1 and CB2 receptors were simultaneously present in pancreatic β and non- β cells, fluorescence amount was greater in β cells in primary cell culture (Figure 2). Presence of both cannabinoid receptors in β and non- β cells is in agreement with previous reports for β ²³⁻²⁵ and α cells^{17,24,26} in rat islets. Expression changes of CB receptors in culture conditions may clarify some discrepancies regarding the cellular type in which these receptors are found. Moreover, this may have implications in functional outcomes of the administration of cannabinoid agonists and antagonists in cellular- and whole-islet cultures. As CB receptors have been found in several cellular types in pancreatic islets, paracrine interactions may also be supported by whole-islet experiments, resulting in contrasting insulin release outcomes reported in the literature.^{12,14,26}

Here, we show that cannabinoid receptors in the pancreatic islet become dysregulated in MetS

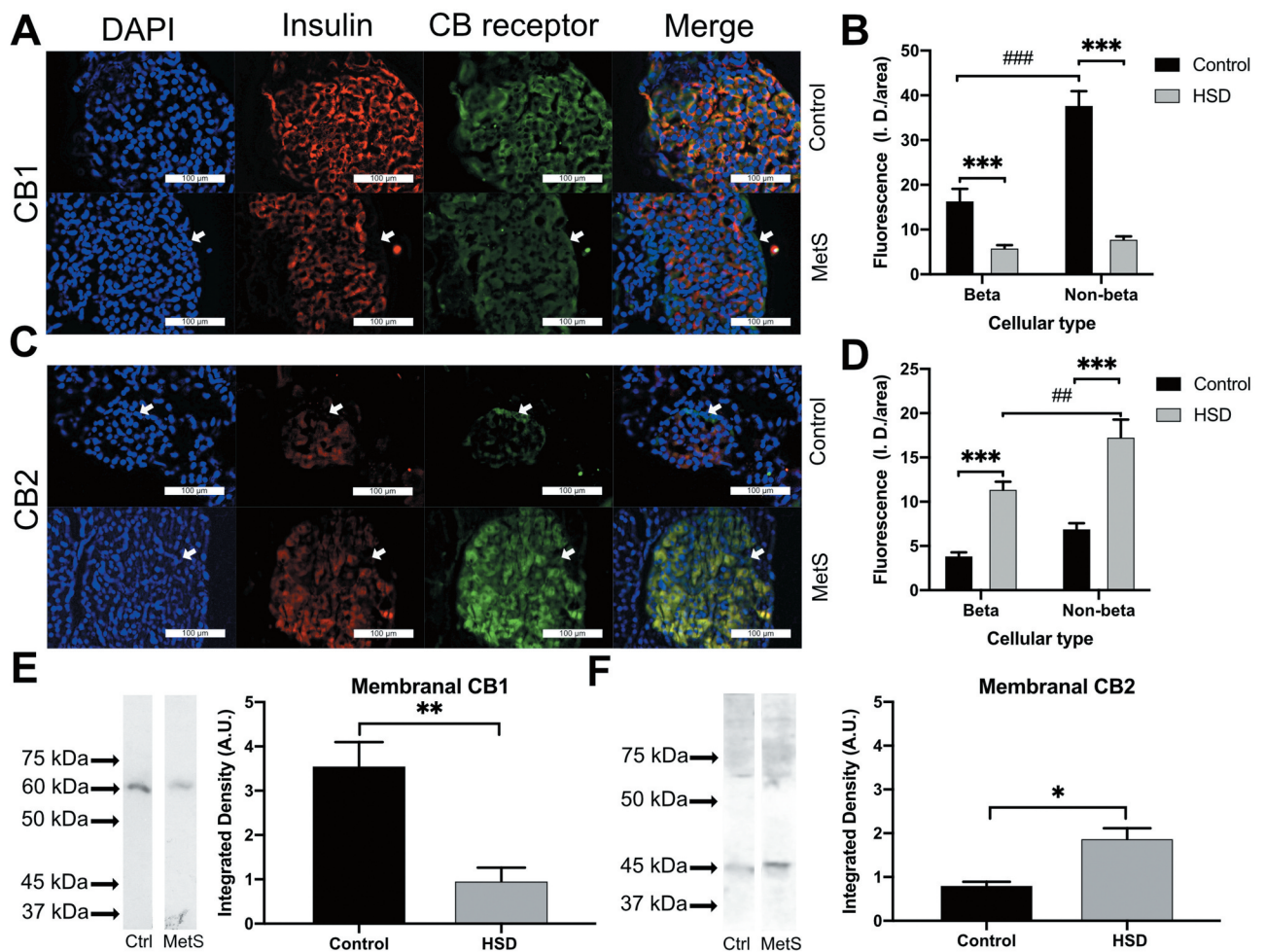


Figure 3. Cannabinoid receptor expression in metabolic syndrome.

The presence of cannabinoid receptors in the control and MetS groups is shown for CB1 in (A) and CB2 in (C). The DAPI-stained cell nuclei are shown in blue in the first column, insulin is shown in red in the second column, and CB receptors in green; the last column shows the merged image. Differences in the intensity of fluorescence between the control and treated groups are shown in (B) for CB1 and (D) for CB2 receptors. (E) shows the difference in the membrane-bound CB1 receptor presence between groups and the molecular weight, control (Ctrl) in the left lane, and MetS in the right lane. (F) shows the difference in the membrane-bound CB2 receptor presence between groups and the molecular weight, control in the left lane, and MetS in the right lane. Arrows highlight the presence of CBs receptors in non- β cells of the periphery of the pancreatic islets. For analysis of the fluorescence differences between groups and cell types, 2-way ANOVA corrected for multiple comparisons with Bonferroni *post hoc* was done. For western blot analysis between groups, unpaired t-tests were done. Results are shown as the mean \pm SEM, differences between treatment groups are shown * $p < .05$, ** $p < .01$, *** $p < .001$, differences between cellular types within the same treatment group are shown ## $p < .01$, ### $p < .001$.

induced by HSD. Notably, the HSD model we used for this work results in blood pressure elevation in addition to dyslipidemia, glucose intolerance, and visceral fat increase.²⁷ These four indicators constitute the central core of MetS.²⁸ CB1 downregulation with concurrent CB2 upregulation was shown by the number of receptors present on the cellular membrane and by the total fluorescence of the cells (Figure 3). These results suggest that, although short-term administration of a fructose-rich diet increases CB1 mRNA expression in pancreatic rat islets,¹⁷ long-term

exposure to hypercaloric diets and subsequent disease development may result in a maladaptive response. In humans, MetS is associated with pancreatic β cell dysfunction.²⁹ This failure of the pancreatic β cell is associated with changes in receptor expression.³⁰ MetS dysregulation of CB1 and CB2 may implicate the participation of the endocannabinoid system in pancreatic β cell diseases. Beyond the pancreatic islet alterations, CB1 and CB2 expression changes have also been reported in tissues expressing both receptor types, such as in diabetic nephropathy and heart

diseases.^{31,32} Furthermore, in the progression from MetS to diabetes mellitus type 2, CB1 receptors present in macrophages also participate in the inflammatory response that contributes to the islet damage.^{33,34}

In the brain, the CB1 receptor provides retrograde negative feedback in GABAergic and glutamatergic synapses,⁵ while CB2 dampens proinflammatory profiles in microglia.³⁵ Cannabinoid receptors appear to participate in the fine-tuning of the cellular response to stimuli. Both cannabinoid receptors, CB1 and CB2, are coupled to $G_{i/o}$ -type G proteins, and their cAMP-lowering effects are sensitive to pertussis toxin.³⁶ However, only CB1 receptors inhibit L-type calcium channels.³⁷ These channels participate in the process of insulin release in pancreatic β cells.³⁸ Accordingly, in the pancreatic islet, CB1-dependent effects include a decrease of cAMP,³⁹ stimulation of glucagon secretion,⁴⁰ and calcium oscillation inhibition.^{24,41} In contrast, CB2-dependent effects include a decrease of cAMP,⁴² with an increase in calcium oscillations.³⁹ Thus, CB1 reduction is expected to counteract the negative regulation that the endocannabinoid system exerts in insulin release, while CB2 upregulation could amplify insulin release. This would be compatible with the presence of hyperinsulinemia without a decreased peripheral response to insulin (Figure 1). We propose that the interplay of CB1 downregulation and CB2 upregulation participates in the insulin release during the early development of MetS. Furthermore, it supports the participation of the endocannabinoid system in the long-term maintenance of normoglycemia.

Our results unveil the ECS regulation under metabolic derangements induced by HSD resulting from pancreatic β cell dysfunction. These findings advance our understanding of the regulation of CB1 and CB2 receptors in pancreatic β cells.

Materials and methods

Ethics statement

The treatment of the animals was carried out subject to the Official Mexican Standard of Technical Specifications for the Production, Care, and Use of Laboratory Animals (NOM-062-ZOO-1999). Procedures were approved by the Ethics and Research Committees of the Faculty

of Medicine at Universidad Nacional Autónoma de México under project 080-2011.

Experimental animals and husbandry

We used eight-week-old male Wistar rats weighing 250–280 grams. They remained under a 12:12 light-dark cycle, at a temperature of $22 \pm 2^\circ\text{C}$, with a relative humidity of 60%, and were pair-housed in plexiglass cages. Laboratory Rodent Diet 5001 (LabDiet) was provided for both groups, and was replenished three times a week, along with fresh bedding and water. All procedures that caused pain were performed under anesthesia with sodium pentobarbital (38 mg/kg), administered intraperitoneally (IP). A dose of intraperitoneal sodium pentobarbital (120 mg/kg) was used at the endpoint for euthanasia. The sample size was calculated by the “resource equation” method.⁴³ Animals were allocated into groups before treatment, after confirming equal weight gain and caloric ingestion for each animal.

Experimental design and MetS induction

Rats ($n = 24$) were given one week to acclimate to colony conditions. Water and food intake was quantified three times a week. Following acclimation, rats were evenly divided into control and HSD groups. The control group had access to water and food *ad libitum*, while the treated HSD group had food access *ad libitum* and water was supplemented with 20% sucrose. This treatment was administered for eight weeks, after which we assessed several MetS components.²⁷ Capillary blood measurements of fasting glucose, triglycerides, and total cholesterol were determined according to the manufacturer’s instructions by colorimetric assay using Accutrend Plus (COBAS, Roche) equipment. Body composition was evaluated through bioimpedance, using an *ad hoc* device that estimates body fat, fat-free mass, extracellular water, and total body water.^{44,45} IPGTT was performed with a dose of 1 g/kg, and the resulting triglyceride curve was recorded.⁴⁶ The ITT was conducted to assert whether the response to insulin was adequate, with a dose of 0.75 UI/kg. Rats were euthanized by IP pentobarbital administration, and blood was obtained from the superior vena cava and

centrifuged to obtain plasma. Samples were frozen and stored at -70°C until processing. An enzyme-linked immunoassay was performed with a Rat High Range Insulin ELISA Kit (ALPCO) following instructions from the manufacturer. Insulin resistance was estimated as follows: $\text{HOMA-IR} = (\text{Fasting glucose} \times \text{Basal insulin})/2,430$, where basal insulin was in microunits per milliliter, and fasting glucose in milligram per deciliter.⁴⁷ Pericardial, epididymal, retroperitoneal and peripancreatic fat pads were retrieved and weighed to estimate visceral adiposity. The pancreas was extracted using the technique described below, and islets for use in western blots were collected in aliquots of 300 islets each.

Pancreatic islet collection and cell culture

For the pancreatic islet obtention and primary cell cultures, we employed a previously described technique.^{48,49} Briefly, the pancreatic duct was localized and cannulated by insufflation with cold Hanks' Balanced Salts Solution (HBSS) supplemented with bovine serum albumin (Microlab), NaHCO_3 (4 mM), HEPES (15 mM), and 1% 100X Antibiotic-Antimycotic (Life Technologies-Thermo Fisher Scientific). The pancreas was removed and transferred to a flask containing HBSS supplemented with collagenase P (0.3 g/L) for incubation at 37°C for 12 min with lateral agitation. After enzymatic digestion, the suspension was washed twice with HBSS by centrifugation at $160 \times g$ for 5 min. Then, the tissue was mechanically disrupted, and the islets were handpicked and rinsed in a clean HBSS solution. For cell culture, islets were dissociated with 1 mL of trypsin-EDTA (2.5X) at 37°C for 3 min. The cell suspension was centrifuged at $160 \times g$ for 5 min and washed twice in RPMI 1640 medium (Life Technologies-Thermo Fisher Scientific) supplemented with fetal bovine serum (FBS, 10%), L-glutamine (1%), and 100X Antibiotic-Antimycotic (1%). Cells were plated on glass coverslips of 4×4 mm coated with poly-L-lysine in polystyrene culture dishes and incubated for 48 h in a humidified atmosphere of 95% O_2 and 5% CO_2 at 37°C . Unless otherwise indicated, all reagents were obtained from Sigma-Aldrich.

Tissue preparation for immunofluorescence

Previously anesthetized control and treated rats were perfused intracardially with 200 mL 0.9%

saline phosphate buffer pH 7.4 (PBS 1X) followed by 400 mL 4% paraformaldehyde in 0.1 M phosphate buffer (pH 7.4). The pancreas was removed and post-fixed overnight in paraformaldehyde fixative at 4°C and then dehydrated in increasing ethanol concentrations overnight and embedded in paraffin wax. The paraffin-embedded pancreas was cut into serial 5- μm thick slices, which were dewaxed and rehydrated according to standard methods. All sections were incubated in a DIVA Decloaker (BioCare Medical) for 15 min at the boiling point to retrieve antigens.

Immunofluorescence

Dual immunofluorescence was performed by the co-incubation of primary insulin antibodies with either a CB1 or CB2 primary antibody, resulting in four groups. Briefly, paraffin-embedded sections and cell cultures were incubated with PBS with 10% bovine serum albumin and 0.3% Triton X100 for 60 min at 20°C . Primary antibodies were incubated overnight at 4°C as follows: CB1 rabbit polyclonal antibody 1:500 (Cayman Chemical Company, cat 10006590), CB2 rabbit polyclonal antibody 1:500 (Santa Cruz Biotechnology Inc., sc-25494), insulin goat polyclonal antibody 1:500 (Santa Cruz Biotechnology Inc., sc-7839). After washing, secondary antibodies were incubated for 2 h at 20°C , AlexaFluor 488 donkey anti-rabbit secondary antibody 1:1000 (Abcam, A-21206) and AlexaFluor 546 donkey anti-goat secondary antibody 1:1000 (Abcam, A-11056). Preparations were mounted with FluoroShield (Abcam, ab104139) according to the manufacturer's instructions. As negative controls, we performed immunofluorescence following the protocols mentioned above, omitting either the primary or secondary antibodies in parallel with the standard procedure.

Western blot

To assess the levels of CB1 or CB2 receptor protein expression, whole pancreatic islets were homogenized in buffer containing protease inhibitors and centrifuged at $600 \times g$ at 4°C for 10 min. The supernatant was centrifuged at $39,000 \times g$ at 4°C for 15 min. The resulting supernatant corresponded to the cytosolic protein fraction and the precipitate to the membrane protein fraction. The resuspended fractions of tissue

homogenates (30 µg protein) were mixed 1:1 with Laemmli buffer and heated (95°C, 5 min) before loading onto a 0.75-mm thick gel. The samples were electrophoresed (150 V, 2 h), and protein was transferred onto a PVDF membrane (Immobilon E, Millipore) at 150 mA for 1 h at 4°C. The membrane was stained with Ponceau's S Red and photographed (G12 camera, Canon),⁵⁰ and each lane was then cut for subsequent incubation. The membrane was washed and incubated with PBS 1X – Tween20 0.3%, 10% nonfat dry milk, and 2% goat normal serum for 30 min at 20°C, and then incubated with anti-CB1 (1:1500; Cayman Chemical Company, cat 10006590), or anti-CB2 (1:500; Santa Cruz Biotechnology, Inc., sc-25494) overnight at 4°C. The blot was washed with PBS-Tween20, incubated for 1 h at 20°C with goat anti-rabbit IgG horseradish peroxidase conjugate (1:2000), and developed with diaminobenzidine (0.5 mg/mL in PBS plus 0.3 µL/mL 30% H₂O₂).

Image acquisition and analysis

Confocal images were taken with a Confocal Zeiss LSM 800 Airyscan microscope, and Zen Blue software, Carl Zeiss Microscopy GmbH, was used. Epifluorescence images were taken with a Nikon Eclipse Ci microscope with Image-Pro Insight with an Evolution, MediaCybernetics camera. To obtain a photographic record of the western blot membrane, a Bio-Rad photodocumenter with a CCD camera was used.⁵¹ FIJI distribution of ImageJ (NIH) was used to assess all images, including the integrated density of staining, area, Ferret diameter, and corrected total fluorescence.⁵² The corrected total fluorescence (CTF) was calculated according to the following formula: CTF = Integrated Density – (Area of selected cell × Mean fluorescence of unspecific background readings).⁵³

Statistical analysis

All data sets were tested for normality with the Shapiro-Wilk test. When suitable, differences between groups were assessed through unpaired t-tests, or when normality assumption was not met Mann-Whitney U tests. For multiple t-tests, Holm-Sidak correction was performed. For comparing time-dependent variables, and when two

factors between groups were considered, two-way ANOVA with Bonferroni *post hoc* analysis for repeated measurements between groups were performed. Results are presented as the mean ± SEM unless otherwise specified. The level of statistical significance was set at $p < .05$ using Prism 8.3 (GraphPad).

Abbreviations

| | |
|-------|--|
| ECS | Endocannabinoid system |
| HSD | High-sucrose diet |
| MetS | Metabolic syndrome |
| CB1 | Cannabinoid receptor 1 |
| CB2 | Cannabinoid receptor 2 |
| IPGTT | Intraperitoneal glucose tolerance test |
| ITT | Insulin tolerance test |

Disclosure of potential conflict of interest

The authors declare that they have no potential conflicts of interest concerning the work described.

Acknowledgments

We thank Carolina Hernández Cruz and Luis Martínez García for their assistance in the animal care and performance of metabolic tests.

Funding

Antonio Barajas-Martínez is a doctoral student from Programa de Doctorado en Ciencias Biomédicas, Universidad Nacional Autónoma de México (UNAM) and received fellowship 596756 from CONACYT. This work was supported by UNAM-DGAPA-PAPIIT IN216119, IA210120, IN228320, and CONACyT 255635.

ORCID

Antonio Barajas-Martínez  <http://orcid.org/0000-0002-5299-0259>

Karina Bermeo  <http://orcid.org/0000-0003-3274-1412>

Lizbeth de la Cruz  <http://orcid.org/0000-0003-1243-2276>

Marina Martínez-Vargas  <http://orcid.org/0000-0002-3729-2161>

Ricardo Jesús Martínez-Tapia  <http://orcid.org/0000-0003-3460-7065>

David Erasmo García  <http://orcid.org/0000-0002-3732-8435>

Luz Navarro  <http://orcid.org/0000-0002-5519-0871>

References

- Maccarrone M, Bab I, Bíró T, Cabral GA, Dey SK, Di Marzo V, Konje JC, Kunos G, Mechoulam R, Pacher P, et al. Endocannabinoid signaling at the periphery: 50 years after THC. *Trends Pharmacol Sci.* 2015;36(5):277–296. doi:10.1016/J.TIPS.2015.02.008.
- Matias I, Di Marzo V. Endocannabinoids and the control of energy balance. *Trends Endocrinol Metab.* 2007;18(1):27–37. doi:10.1016/j.tem.2006.11.006.
- Jourdan T, Godlewski G, Kunos G. Endocannabinoid regulation of β -cell functions: implications for glycaemic control and diabetes. *Diabetes, Obes Metab.* 2016;18(6):549–557. doi:10.1111/dom.12646.
- Kim W, Doyle ME, Liu Z, Lao Q, Shin Y, Carlson OD, Kim HS, Thomas S, Napora JK, Lee EK, et al. Cannabinoids inhibit insulin receptor signaling in. *Diabetes.* 2011;1(13):1–12. doi:10.2337/db10-1550.
- Ruehle S, Rey AA, Remmers F, Lutz B. The endocannabinoid system in anxiety, fear memory and habituation. *J Psychopharmacol.* 2012;26(1):23–39. doi:10.1177/0269881111408958.
- Koch M. Cannabinoid receptor signaling in central regulation of feeding behavior: a mini-review. *Front Neurosci.* 2017;11:293. doi:10.3389/fnins.2017.00293.
- Osei-Hyiaman D, DePetrillo M, Pacher P, Liu J, Radaeva S, Bátkai S, Harvey-White J, Mackie K, Offertáler L, Wang L, et al. Endocannabinoid activation at hepatic CB1 receptors stimulates fatty acid synthesis and contributes to diet-induced obesity. *J Clin Invest.* 2005;115(5):1298–1305. doi:10.1172/JCI23057.
- Bermúdez-Siva FJ, Serrano A, Diaz-Molina FJ, Sánchez Vera I, Juan-Pico P, Nadal A, Fuentes E, Rodríguez De Fonseca F. Activation of cannabinoid CB1 receptors induces glucose intolerance in rats. *Eur J Pharmacol.* 2006;531(1–3):282–284. doi:10.1016/j.ejphar.2005.12.016.
- Schaich CL, Shaltout HA, Brosnihan KB, Howlett AC, Diz DI. Acute and chronic systemic CB1 cannabinoid receptor blockade improves blood pressure regulation and metabolic profile in hypertensive (mRen2)27 rats. *Physiol Rep.* 2014;2(8):e12108. doi:10.14814/phy2.12108.
- Alshaarawy O, Anthony JC. Cannabis smoking and diabetes mellitus: results from meta-analysis with eight independent replication samples. *Epidemiology.* 2015;26(4):597–600. doi:10.1097/EDE.0000000000000314.
- Imtiaz S, Rehm J. The relationship between cannabis use and diabetes: results from the national epidemiologic survey on alcohol and related conditions III. *Drug Alcohol Rev.* 2018;37(7):897–902. doi:10.1111/dar.12867.
- Bermúdez-Silva FJ, Suárez J, Baixeras E, Cobo N, Bautista D, Cuesta-Muñoz AL, Fuentes E, Juan-Pico P, Castro MJ, Milman G, et al. Presence of functional cannabinoid receptors in human endocrine pancreas. *Diabetologia.* 2008;51(3):476–487. doi:10.1007/s00125-007-0890-y.
- González-Mariscal I, Montoro RA, Doyle ME, Liu Q-R, Rouse M, O'Connell JF, Santa-Cruz Calvo S, Krzyślik Walker SM, Ghosh S, Carlson OD, et al. Absence of cannabinoid 1 receptor in beta cells protects against high-fat/high-sugar diet-induced beta cell dysfunction and inflammation in murine islets. *Diabetologia.* 2018;61(6):1470–1483. doi:10.1007/s00125-018-4576-4.
- Juan-Picó P, Fuentes E, Bermúdez-Silva FJ, Javier Díaz-Molina F, Ripoll C, Rodríguez de Fonseca F, Nadal A. Cannabinoid receptors regulate Ca(2+) signals and insulin secretion in pancreatic beta-cell. *Cell Calcium.* 2006;39(2):155–162. doi:10.1016/j.ceca.2005.10.005.
- Spivak CE, Kim W, Liu QR, Lupica CR, Doyle ME. Blockade of β -cell KATP channels by the endocannabinoid, 2-arachidonoylglycerol. *Biochem Biophys Res Commun.* 2012;423(1):13–18. doi:10.1016/j.bbrc.2012.05.042.
- Vilches-Flores A, Delgado-Buenrostro NL, Navarrete-Vázquez G, Villalobos-Molina R. CB1 cannabinoid receptor expression is regulated by glucose and feeding in rat pancreatic islets. *Regul Pept.* 2010;163(1–3):81–87. doi:10.1016/j.regpep.2010.04.013.
- Flores LE, Alzugaray E, Cubilla MA, Mari P, Del ZH, Roma CL. Islet cannabinoid receptors: cellular distribution and biological function. *Pancreas.* 2013;42(7):1085–1092.
- Alberti KGMM, Eckel RH, Grundy SM, Zimmet PZ, Cleeman JJ, Donato KA, Fruchart JC, James WPT, Loria CM, Smith SC. Harmonizing the metabolic syndrome: A joint interim statement of the international diabetes federation task force on epidemiology and prevention; National heart, lung, and blood institute; American heart association; World heart federation; International. *Circulation.* 2009;120(16):1640–1645. doi:10.1161/CIRCULATIONAHA.109.192644.
- González-Mariscal I, Egan JM. Endocannabinoids in the Islets of Langerhans: the ugly, the bad, and the good facts. *Am J Physiol Metab.* 2018;315(2):E174–E179. doi:10.1152/ajpendo.00338.2017.
- Crespillo A, Suárez J, Bermúdez-Silva FJ, Rivera P, Vida M, Alonso M, Palomino A, Lucena MA, Serrano A, Pérez-Martín M, et al. Expression of the cannabinoid system in muscle: effects of a high-fat diet and CB₁ receptor blockade. *Biochem J.* 2011;433(1):175LP–185. <http://www.biochemj.org/content/433/1/175.abstract>.
- Deveaux V, Cadoudal T, Ichigotani Y, Teixeira-Clerc F, Louvet A, Manin S, Nhieu JT-V, Belot MP, Zimmer A, Even P, et al. Cannabinoid CB2 receptor potentiates obesity-associated inflammation, insulin resistance and hepatic steatosis. *PLoS One.* 2009;4(6):e5844. doi:10.1371/journal.pone.0005844.
- Starowicz KM, Cristino L, Matias I, Capasso R, Racioppi A, Izzo A, Di Marzo V. Endocannabinoid dysregulation in the pancreas and adipose tissue of mice fed with a high-fat diet. *Obesity (Silver Spring).* 2008;16(3):553–565. doi:10.1038/oby.2007.106.
- De Petrocellis L, Marini P, Matias I, Moriello AS, Starowicz K, Cristino L, Nigam S, Di Marzo V. Mechanisms for the coupling of cannabinoid receptors

- to intracellular calcium mobilization in rat insulinoma beta-cells. *Exp Cell Res.* 2007;313(14):2993–3004. doi:10.1016/j.yexcr.2007.05.012.
24. Bermudez-Silva FJ, Sanchez-Vera I, Suárez J, Serrano A, Fuentes E, Juan-Pico P, Nadal A, Rodríguez de Fonseca F. Role of cannabinoid CB2 receptors in glucose homeostasis in rats. *Eur J Pharmacol.* 2007;565(1–3):207–211. doi:10.1016/j.ejphar.2007.02.066.
 25. Malenczyk K, Jazurek M, Keimpema E, Silvestri C, Janikiewicz J, Mackie K, Di Marzo V, Redowicz MJ, Harkany T, Dobrzyn A. CB1 cannabinoid receptors couple to focal adhesion kinase to control insulin release. *J Biol Chem.* 2013;288(45):32685–32699. doi:10.1074/jbc.M113.478354.
 26. Pico PJ, Pico PJ, Ropero AB, Ana B, Tuduri E, De RPicó P, Ropero A, Tudurí E, Quesada I, Fuentes E, Bermudez-Silva F, et al. Regulation of glucose - induced [Ca²⁺]_i signals by cannabinoid CB1 and CB2 receptors in pancreatic alpha - and delta - cells within intact islets of Langerhans. *Obesity Metab.* 2009;5(1):20–28.
 27. Larqué C, Velasco M, Navarro-Tableros V, Duhne M, Aguirre J, Gutiérrez-Reyes G, Moreno J, Robles-Diaz G, Hong E, Hiriart M. Early endocrine and molecular changes in metabolic syndrome models. *IUBMB Life.* 2011;63(10):831–839. doi:10.1002/iub.544.
 28. Huang PL. A comprehensive definition for metabolic syndrome. *Dis Model Mech.* 2009;2(5–6):231–237. doi:10.1242/dmm.001180.
 29. Malin SK, Finnegan S, Fealy CE, Filion J, Rocco MB, Kirwan JP. β -Cell dysfunction is associated with metabolic syndrome severity in adults. *Metab Syndr Relat Disord.* 2014;12(2):79–85. doi:10.1089/met.2013.0083.
 30. Medina-Gomez G, Yetukuri L, Velagapudi V, Campbell M, Blount M, Jimenez-Linan M, Ros M, Oresic M, Vidal-Puig A. Adaptation and failure of pancreatic beta cells in murine models with different degrees of metabolic syndrome. *Dis Model Mech.* 2009;2(11–12):582–592. doi:10.1242/dmm.003251.
 31. Gruden G, Barutta F, Kunos G, Pacher P. Role of the endocannabinoid system in diabetes and diabetic complications. *Br J Pharmacol.* 2016;173(7):1116–1127. doi:10.1111/bph.13226.
 32. Cappellano G, Uberti F, Caimmi PP, Pietronave S, Mary DASGSG, Dianzani C, Micalizzi E, Melensi M, Boldorini R, Nicosia G, et al. Different expression and function of the endocannabinoid system in human epicardial adipose tissue in relation to heart disease. *Can J Cardiol.* 2013;29(4):499–509. doi:10.1016/j.cjca.2012.06.003.
 33. Jourdan T, Szanda G, Cinar R, Godlewski G, Holovac DJ, Park JK, Nicoloso S, Shen Y, Liu J, Rosenberg AZ, et al. Developmental role of macrophage cannabinoid-1 receptor signaling in type 2 diabetes. *Diabetes.* 2017;66(4):994–1007. doi:10.2337/db16-1199.
 34. Jourdan T, Godlewski G, Cinar R, Bertola A, Szanda G, Liu J, Tam J, Han T, Mukhopadhyay B, Skarulis MC, et al. Activation of the Nlrp3 inflammasome in infiltrating macrophages by endocannabinoids mediates beta cell loss in type 2 diabetes. *Nat Med.* 2013;19(9):1132–1140. doi:10.1038/nm.3265.
 35. Malek N, Popiolek-Barczyk K, Mika J, Przewlocka B, Starowicz K. Anandamide, acting via CB2 receptors, alleviates LPS-induced neuroinflammation in rat primary microglial cultures. *Neural Plast.* 2015;2015:130639. doi:10.1155/2015/130639.
 36. Felder CC, Joyce KE, Briley EM, Mansouri J, Mackie K, Blond O, Lai Y, Ma AL, Mitchell RL. Comparison of the pharmacology and signal transduction of the human cannabinoid CB1 and CB2 receptors. *Mol Pharmacol.* 1995;48:443–450.
 37. Qian W-J, Yin N, Gao F, Miao Y, Li Q, Li F, Sun X-H, Yang X-L, Wang Z. Cannabinoid CB1 and CB2 receptors differentially modulate L- and T-type Ca²⁺ channels in rat retinal ganglion cells. *Neuropharmacology.* 2017;124:143–156. doi:10.1016/J.NEUROPHARM.2017.04.027.
 38. Braun M, Ramracheya R, Bengtsson M, Zhang Q, Karanaukaite J, Partridge C, Johnson PR, Rorsman P. Voltage-Gated Ion Channels in Human Pancreatic B-Cells: electrophysiological Characterization and Role in Insulin Secretion. *Diabetes.* 2008;57(6):1618–1628. doi:10.2337/db07-0991.M.B.
 39. Li C, Jones PM, Persaud SJ. Cannabinoid receptors are coupled to stimulation of insulin secretion from mouse MIN6 beta-cells. *Cell Physiol Biochem.* 2010;26(2):187–196. doi:10.1159/000320527.
 40. Bermúdez-Silva FJ, Suárez Pérez J, Nadal A, Rodríguez de Fonseca F, Bermudez-Silva FJ, Suarez Perez J, Rodriguez de Fonseca F. The role of the pancreatic endocannabinoid system in glucose metabolism. *Best Pr Res Clin Endocrinol Metab.* 2009;23(1):87–102.
 41. Nakata M, Yada T. Cannabinoids inhibit insulin secretion and cytosolic Ca²⁺ oscillation in islet β -cells via CB1 receptors. *Regul Pept.* 2008;145(1–3):49–53. doi:10.1016/j.regpep.2007.08.009.
 42. González-Mariscal I, Krzysik-Walker SM, Kim W, Rouse M, Egan JM. Blockade of cannabinoid 1 receptor improves GLP-1R mediated insulin secretion in mice. *Mol Cell Endocrinol.* 2016;423:1–10. doi:10.1016/j.mce.2015.12.015.
 43. Charan J, Kantharia N. How to calculate sample size in animal studies? *J Pharmacol Pharmacother.* 2013;4(4):303–306. doi:10.4103/0976-500X.119726.
 44. Bermeo K. Indicadores conductuales tempranos en el desarrollo del síndrome metabólico en rata [Thesis]. Ciudad de México, México: Universidad Nacional Autónoma de México, 2013. <http://132.248.9.195/ptd2013/septiembre/0701079/Index.html#Textocompleto>.
 45. Rutter K, Hennoste L, Ward LC, Cornish BH, Thomas BJ. Bioelectrical impedance analysis for the estimation of body composition in rats. *Lab Anim.* 1998;32(1):65–71. doi:10.1258/002367798780559356.

46. Lomba A, Milagro FI, García-Díaz DF, Martí A, Campián J, Martínez JA. Obesity induced by a pair-fed high fat sucrose diet: methylation and expression pattern of genes related to energy homeostasis. *Lipids Health Dis.* 2010;9(1):60. doi:10.1186/1476-511X-9-60.
47. Cacho J, Sevillano J, De Castro J, Herrera E, Ramos MP. Validation of simple indexes to assess insulin sensitivity during pregnancy in Wistar and Sprague-Dawley rats. *Am J Physiol - Endocrinol Metab.* 2008;295(5):5. doi:10.1152/ajpendo.90207.2008.
48. de la Cruz L, Puente EI, Reyes-Vaca A, Arenas I, Garduño J, Bravo-Martínez J, Garcia DE. PIP2 in pancreatic β -cells regulates voltage-gated calcium channels by a voltage-independent pathway. *Am J Physiol Physiol.* 2016;311(4):C630–C640. doi:10.1152/ajpcell.00111.2016.
49. Velasco M, Larqué C, Díaz-García CM, Sanchez-Soto C, Hiriart M. Rat pancreatic beta-cell culture. In: *Methods in molecular biology*. Vol. 1727. Humana Press Inc; 2018. p. 261–273. doi:10.1007/978-1-4939-7571-6_20.
50. Romero-calvo I, Ocón B, Martínez-moya P, Suárez MD, Zarzuelo A, Martínez-augustin O, Medina FSD. Reversible Ponceau staining as a loading control alternative to actin in Western blots. *Anal Biochem.* 2010;401(2):318–320. doi:10.1016/j.ab.2010.02.036.
51. Gassmann M, Rohde B. Quantifying western blots: pitfalls of densitometry. *Electrophoresis.* 2009;1845–1855. doi:10.1002/elps.200800720.
52. Arqués O, Chicote I, Tenbaum S, Puig I, Palmer G. Standardized relative quantification of immunofluorescence tissue staining. *Protoc Exch.* 2012 Apr. doi:10.1038/protex.2012.008
53. Gavet O, Pines J. Progressive activation of CyclinB1-Cdk1 coordinates entry to mitosis. *Dev Cell.* 2010;18(4):533–543. doi:10.1016/j.devcel.2010.02.013.